

Experiments on arrays of globally coupled chaotic electrochemical oscillators: Synchronization and clustering

Wen Wang, István Z. Kiss,^{a)} and J. L. Hudson

Department of Chemical Engineering, Thornton Hall, University of Virginia, Charlottesville, Virginia 22903-2442

(Received 1 September 1999; accepted for publication 19 October 1999)

Experiments on chaotically oscillating arrays of 64 nickel electrodes in sulfuric acid were carried out. External resistors in parallel and series are added to vary the extent of global coupling among the oscillators without changing the other properties of the system. The array is heterogeneous due to small variations in the properties of the electrodes and there is also a small amount of noise. The addition of global coupling transforms a system of independent elements to a state of complete synchronization. At intermediate coupling strengths stable clusters, or condensates of elements, form. All the elements in a cluster follow the same chaotic trajectory but each cluster has its own dynamics; the system is thus temporally chaotic but spatially ordered. Many cluster configurations occur under the same conditions and transitions among them can be produced. For values of the coupling parameter on either side of the stable cluster region a non-stationary behavior occurs in which clustered and synchronized states alternately form and break up. Some statistical properties of the cluster states are determined. © 2000 American Institute of Physics.

[S1054-1500(00)01601-3]

We present experimental results on the characteristics of globally coupled chaotic electrochemical oscillators. An experimental design has been developed in which the global coupling can be varied without changing the local dynamics or rate of reaction through alterations in other conditions. There are two aspects to the work. First is the presentation of results from a laboratory experiment on phenomena such as synchronization and condensation or cluster formation to which the large number of theoretical studies on arrays of coupled maps or differential equations can be compared. The experimental system, of course, has a certain amount of heterogeneity and noise. The second aspect has direct electrochemical implications. The array of electrodes behaves qualitatively like a larger single surface and information on spatiotemporal pattern formation in electrochemically reacting systems is thus obtained.

I. INTRODUCTION

Coupling of periodic and chaotic oscillators is a subject of considerable current interest. Many theoretical studies of coupled maps,¹⁻⁹ neural networks,¹⁰ and sets of ordinary differential equations¹¹⁻¹⁸ have been carried out. Coupling of periodic oscillators can produce a synchronized state in which the oscillators follow the same state-space trajectories.¹⁹ Synchronization also occurs in the coupling of chaotic oscillators.

Global coupling in sets of chaotic oscillators can also lead to condensation or clustering in which subgroups of the

oscillators are synchronized. Without noise the states of oscillators in the clusters are identical whereas in noisy or heterogeneous systems the elements in a cluster remain close to each other. Such behavior has been studied in detail by Kaneko for coupled map systems¹⁻³ and more recently by Zanette and Mikhailov for sets of differential equations.¹¹

Laboratory studies of clustering and synchronization, in which a control parameter is varied without changing the inherent dynamics of the individual elements, are lacking. In the present paper we report the results of experimental studies on globally coupled electrochemical oscillators. The work follows a recent related paper on coupled limit cycle oscillators.²⁰ Although care was taken to make each element of the array in the same manner and to reduce noise, there is, as in all experimental systems, a certain amount of heterogeneity and noise. Comparisons are made between these results and some of the theoretical studies and simulations cited above. We note that clustering appears even in arrays of a few elements and that the 64-element array exhibits many of the statistical characteristics seen in the theoretical studies done with larger array sizes.

The influence of global coupling on spatiotemporal pattern formation is often important in biological and chemical reacting systems. For example, in gas-solid systems mixing in the gas phase produces a global coupling because a consumption of reactants or production of products at one location causes changes in conditions at all locations of the system.²¹ Such coupling can have a strong role in altering pattern formation.²² In electrochemical systems a nonlocal coupling among reactive sites arises through the electric field; potential changes at some location are transmitted rapidly to other locations.²³⁻²⁷ This coupling is long-range but is not global because its effect dies out with increasing distance. In addition, a global coupling can be imposed on elec-

^{a)}Permanent address: Institute of Physical Chemistry, Kossuth Lajos University, Debrecen H-4010, Hungary.

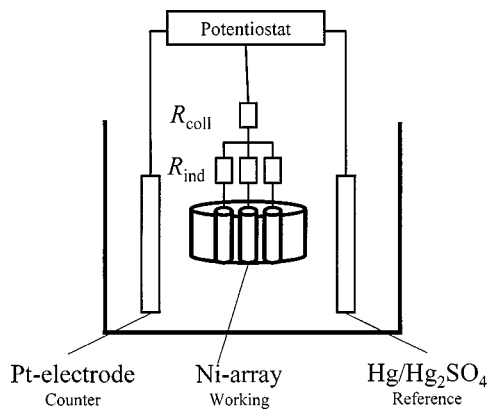


FIG. 1. Experimental setup.

trochemical systems simply through the addition of an external resistance.²⁸

One method of determining the spatiotemporal structure in the electrochemical systems is with the use of electrode arrays.^{29,30} The arrays consist of a number of small disks that are made from the end of wires embedded in an insulator. One advantage of the arrays is that the individual currents can be measured and thus the rate of reaction as a function of position and time can be found. Since the coupling is largely long-range and through the electrolyte, an array can exhibit overall behavior that is similar to that of a single electrode of the same total area.^{30,31}

In the present work we investigate the influence of global coupling on the chaotic electrodisolution of an array of electrodes. In electrochemical systems the coupling strengths can be varied by changing the concentration of the electrolyte and by variations of the cell geometry. However, in making either of these changes the potential drop across the electrical double layer would also be changed. In this work we employ a method of altering the strength of global coupling while holding all other parameters constant. This is done through the use of external resistors; the total external resistance is held constant while the fraction dedicated to individual currents, as opposed to the total current, can be varied. Since the electrolyte concentration is high, the external resistance is larger than that of the electrolyte and the added global coupling dominates over the non-global coupling inherent in the system.

II. EXPERIMENTS

A. Apparatus and experimental conditions

The arrays are made up of 64 electrodes in an 8×8 geometry. The electrodes are made from pure Ni wire (Aldrich Chemical Co., 99.99+%) of diameter 1 mm. The electrodes are embedded in epoxy and reaction takes place only at the ends.

The electrode array was used as a working electrode in a standard electrochemical cell shown in Fig. 1. For convenience only a three-electrode array is shown. All electrodes in the array are held at the same constant potential with a potentiostat; in all the experiments reported here the applied potential was 1.355 V ($\text{Hg}/\text{Hg}_2\text{SO}_4/\text{K}_2\text{SO}_4$). The electrodes

are connected to the potentiostat through one collective resistor and through individual resistors connected to each of the electrodes. Zero resistance ammeters (ZRA's) were used to measure the currents of the electrodes independently. The ZRA circuitry was inserted between the individual and collective resistors. The data acquisition was done at 200 Hz for all data shown.

Experiments were carried out in 4.5 M H_2SO_4 solution directly diluted from 5 M sulfuric acid. N_2 was bubbled through the solution for half an hour prior to each experiment. The counter electrode is Pt sheet. The cell was held at 11 °C.

Further details can be found in an earlier paper.²⁰

B. Coupling parameter

There are two ways of connecting the external resistors to a multielectrode cell (see Fig. 1): individually (R_{ind}) and collectively (R_{coll}). A total resistance (R_{tot}) is defined as

$$R_{\text{tot}} = R_{\text{coll}} + \frac{R_{\text{ind}}}{n}, \quad (1)$$

where n is the number of electrodes. In these experiments $R_{\text{tot}} = 14.2 \Omega$.

The collective resistor couples the electrodes globally: the current on one electrode affects the dynamics of the other electrodes since current through any given electrode influences the potential drop on all electrodes equally. The collective resistance fraction (ε) expresses the fraction of total collective resistance:

$$\varepsilon = \frac{R_{\text{coll}}}{R_{\text{tot}}}. \quad (2)$$

This value of ε provides a convenient way of expressing the global coupling in the system. If $\varepsilon = 0$, the external resistance furnishes no additional global coupling. If $\varepsilon = 1$, maximal external global coupling is achieved. Thus we have an (added) global coupling parameter that takes on values from zero to one as the global coupling increases.

C. Heterogeneities, noise, and base-line coupling

Although care was taken in construction of the apparatus and also during the experiments, there is intrinsically a certain amount of heterogeneity and noise. In addition, even without added coupling there is a small amount of coupling inherent in the system. This coupling comes through potential drops in the electrolyte and in the external circuitry. In our case these are low and small compared to the added global coupling.

Some information on the amount of heterogeneity and noise can be seen in the results of some recent experiments on coupled harmonic oscillators on the same array configuration.²⁰ For no added global coupling ($\varepsilon = 0.0$) the 64 almost independently periodically oscillating electrodes had a mean frequency of 1.44 Hz with a standard deviation of about 0.02 Hz. (We did not have enough resolution to determine the exact distribution of the frequencies; it is not

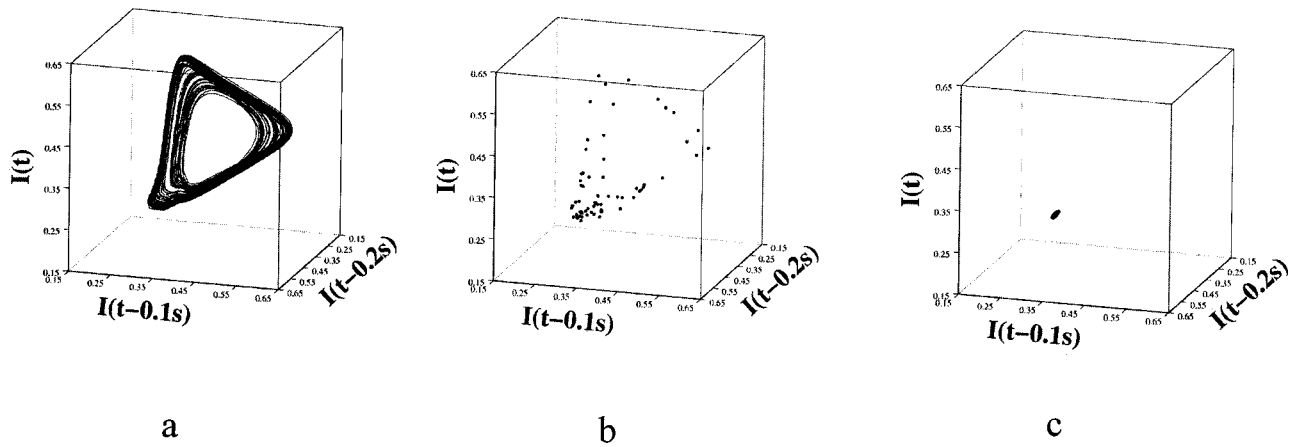


FIG. 2. (a) Attractor constructed with the time series of the single electrode. $\varepsilon=0.0$. (b) Snapshot of position in state space constructed from currents of all 64 electrodes, $\varepsilon=0.0$. (c) Snapshot of position in state space constructed from currents of all 64 electrodes, $\varepsilon=1.0$.

quite symmetrical about the mean but rather somewhat skewed toward the higher frequencies.) As the global coupling was increased the frequency distribution becomes less broad and at $\varepsilon=0.11$ the behavior becomes synchronized; all

oscillators have the same frequency. Even at synchronization, however, they were not yet in phase. At a global coupling of $\varepsilon=0.17$ the phases became identical to within the resolution of the experiment.

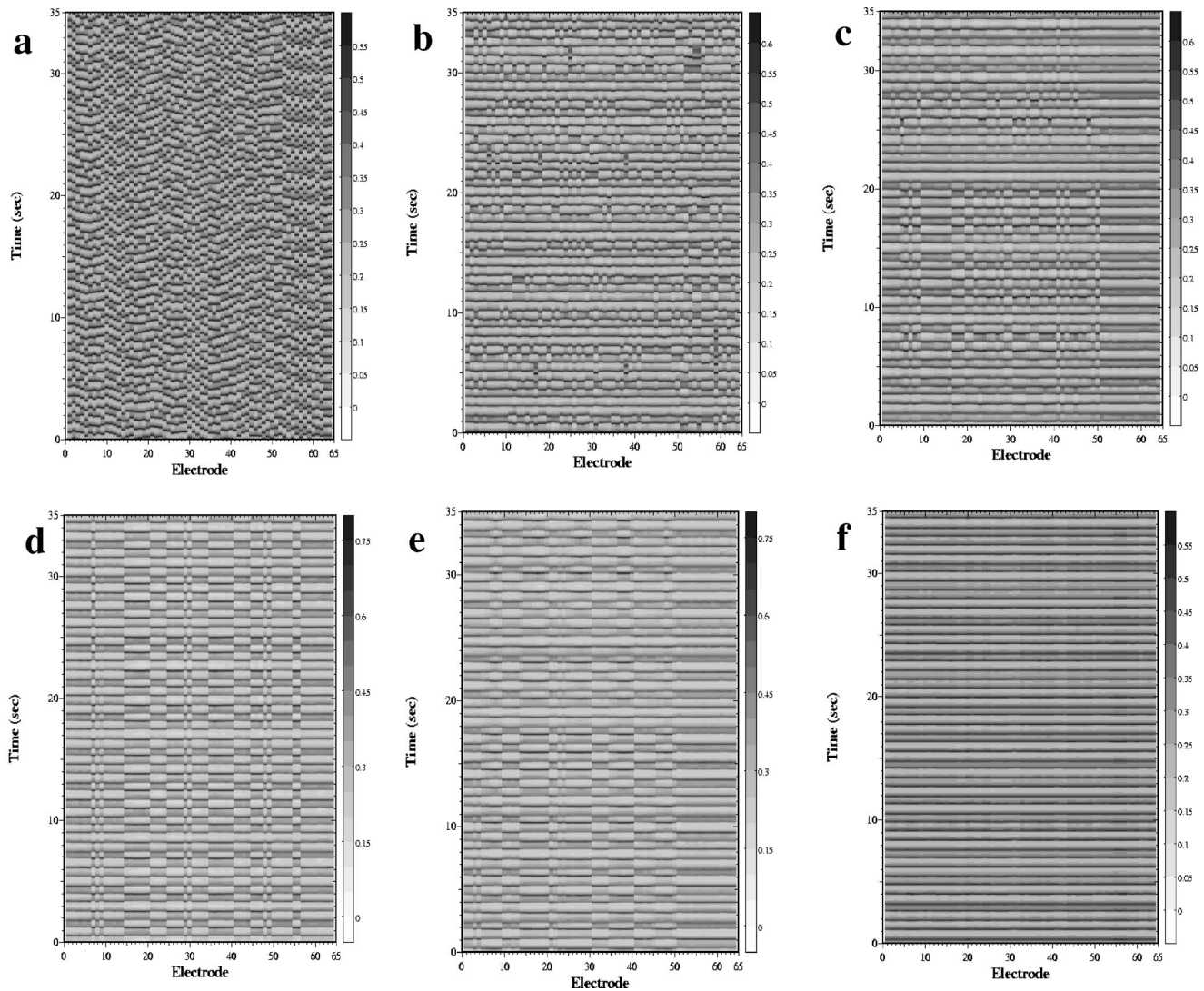


FIG. 3. Space/time plot of the local currents; dark corresponds to high current. (a) $\varepsilon=0$, (b) $\varepsilon=0.34$, (c) $\varepsilon=0.67$, (d) $\varepsilon=0.725$, (e) $\varepsilon=0.78$, (f) $\varepsilon=1.0$.

III. RESULTS

An attractor, reconstructed from the time series of an individual electrode under conditions of no global coupling ($\varepsilon=0$), is shown in Fig. 2(a). The behavior is that of a low-dimensional chaotic attractor. (The information dimension was calculated to be approximately 2.2.) Although there is some inherent coupling in the system, even when $\varepsilon=0$, this coupling is weak. Nearby trajectories of two of the individual oscillators diverge in a few oscillations.

Snapshots of the position in state space for all 64 electrodes are shown in Figs. 2(b) and 2(c) for no global coupling and maximal global coupling respectively. Note in Fig. 2(b) that the points fill a region in state space that has the same size as that of the attractor for an individual element. The points are essentially distributed over the entire range of possible locations as would be expected for the case of very weak coupling. For maximal coupling, Fig. 2(c), the points all lie in a small ball on the attractor; these points move as an entity through state space. Since noise is present in the system and since the elements are not identical, two time series can never become identical; we thus say that the oscillators are synchronized if the distance in state space is below some given value.

Space-time plots for several values of the coupling parameter are shown in Fig. 3; the dark shading corresponds to higher current. The results with no added global coupling are seen in Fig. 3(a). Spatial structuring begins as the coupling strength is increased somewhat [Fig. 3(b)]. For maximal coupling synchronization is seen [Fig. 3(f)]. At intermediate values of the coupling strength ($\varepsilon=0.725$) clusters form; one of the many stable cluster configurations can be seen in Fig. 3(d). Transient cluster regions occur on both sides of the stable cluster region, that is for coupling strengths less than and also greater than that at which stable clusters form; two such transient cluster regions are shown in Figs. 3(c) and 3(e).

In the 64-electrode system many cluster configurations are possible. We have observed clusters with as few as 18 elements. The observed range is thus (18,46) to (32,32). Although it is of course possible that stable clusters occur outside that range, it appears likely that they are unstable since they have not been observed in a large number of experiments. Note that Kaneko has found a finite range of stable two-cluster configurations in this studies with coupled maps.^{1,2} A few of the cluster configurations are shown in Fig. 4. We show these configurations in order to give an indication of the influence of the relatively small (but not zero) coupling that is inherent in the system and that exists even without the added coupling. Note in the configurations of Fig. 4 that the edge elements have a tendency to be in the same cluster. Coupling among these edge regions is somewhat stronger than it is among elements in the interior of the array.

The cluster configuration reached in any given experiment of course depends on the initial conditions. There is a sufficiently large number of possible configurations such that we have never attained the exact same arrangement; by the same arrangement we mean not only that the cluster sizes are

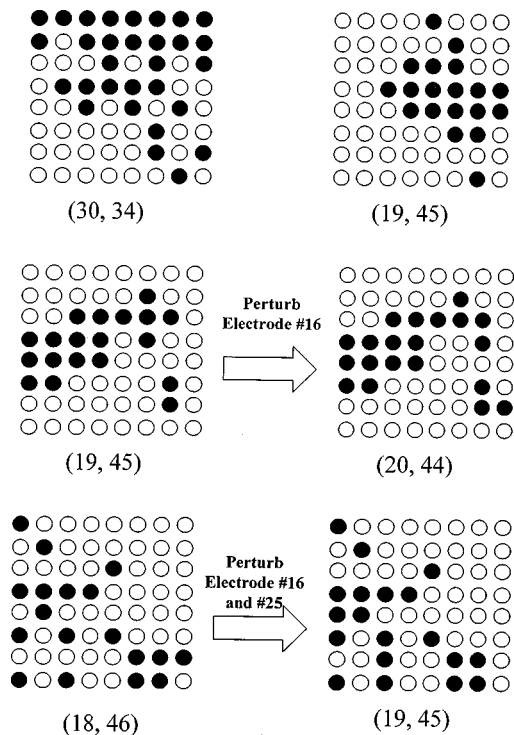


FIG. 4. Some of the many possible cluster arrangements. Some transitions due to perturbations are also shown. Electrodes numbered from lower left, starting across.

the same but also that the exact same individual elements exist in each of the clusters. In Fig. 4 three different (19,45) cluster arrangements are shown. In the experiment there is an initial transient of about 30 seconds after which the stationary state is reached. The cluster configurations in this stationary state are all then very stable. Once a state is attained, the system remains in that state.

A moderate disturbance will produce a transient followed by a return to the same cluster configuration. It is possible with sufficiently large disturbances to change the cluster configurations. (The disturbances are induced by breaking the circuit for short times.) A few such transitions are shown. The disturbances are made on either one or two of the electrodes. The resulting change may or may not occur in the electrode being perturbed. Because of the stability of the cluster arrangements, we have only been able to induce transitions in which the number of elements in the respective clusters changes by one. For example, transitions from a (19,45) state to a (20,44) and also from (20,44) to (19,45) are shown. This is not to say that only one element changes its position in the cluster. Transitions have been observed with perturbations in which three elements change their position but in which the net change is only one such as is seen in the last perturbation experiment shown in Fig. 4.

Time series of the individual elements and of the total current (sum of 64) and the attractors reconstructed from them differ among the cluster configurations. Attractors are shown in Figs. 5(a) and 5(b) for two of the cluster configurations. The differences among the six attractors can be seen. Other cluster configurations have their own dynamics. We note that the attractors constructed for the individual elements are on two bands; this two-band structure was seen in

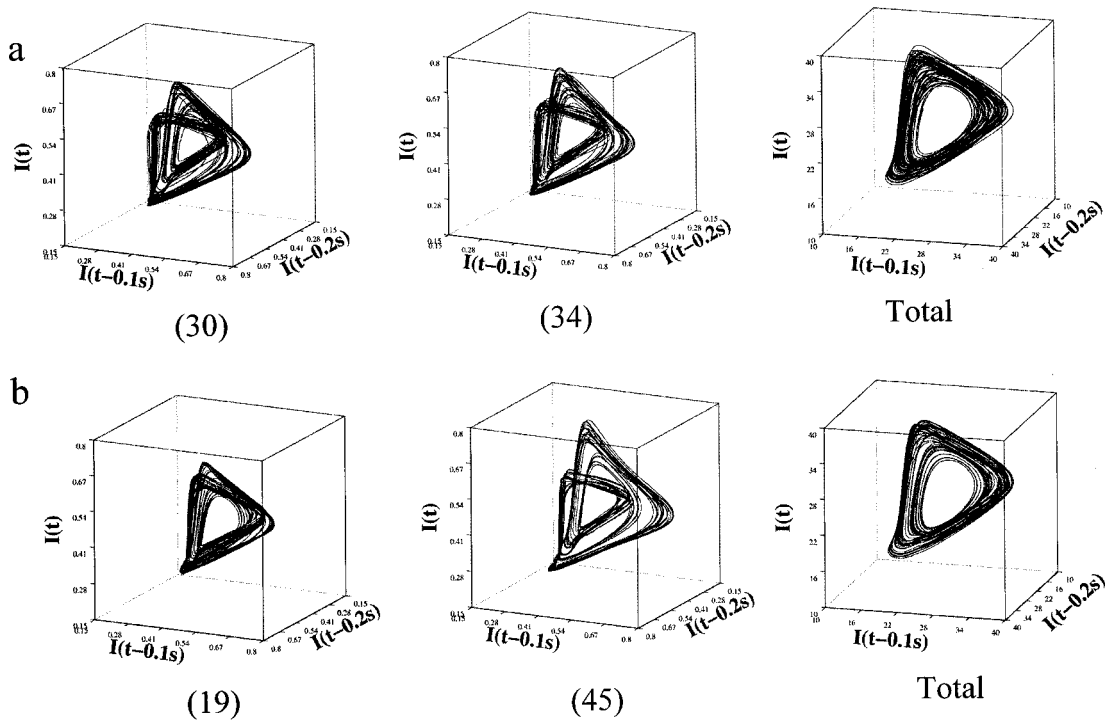


FIG. 5. (a) Attractors for individual and total currents, (30,34) cluster, Delay time=0.1 s. (b) Attractors for individual and total currents, (19,45) cluster. $\epsilon = 0.725$.

every experiment in the cluster region. However, the two-band structure is not apparent in the dynamics of the total current.

The behavior of the two clusters can perhaps best be seen in the snapshots of the position in state-space of each of the 64 elements taken at a series of times. Such snapshots in

the cluster region for one stable cluster configuration (23,41) can be seen in Fig. 6. Note that the elements remain in their respective cluster. These clusters change shapes somewhat as they move through state space. Occasionally the noise is strong enough to drive one element (see $t = 20$ s) out of its cluster but this element quickly returns to its cluster. Further-

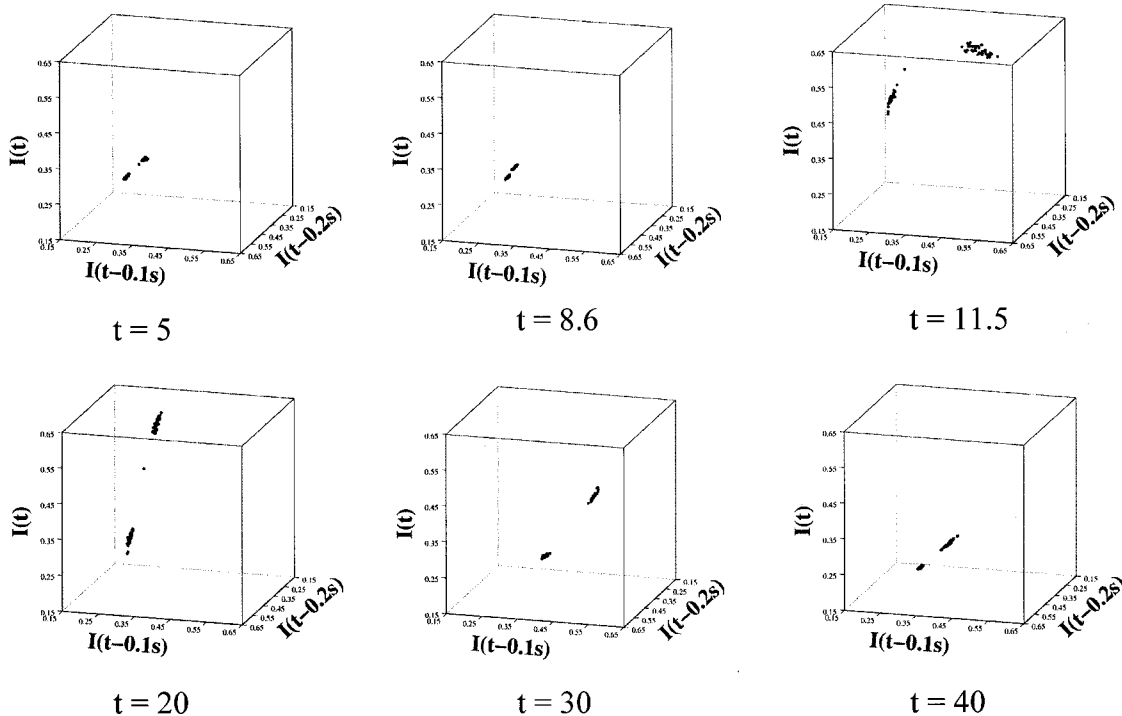


FIG. 6. Snapshots of position in state space for each of the 64 elements. (23,41) stable clusters at $\epsilon = 0.725$.

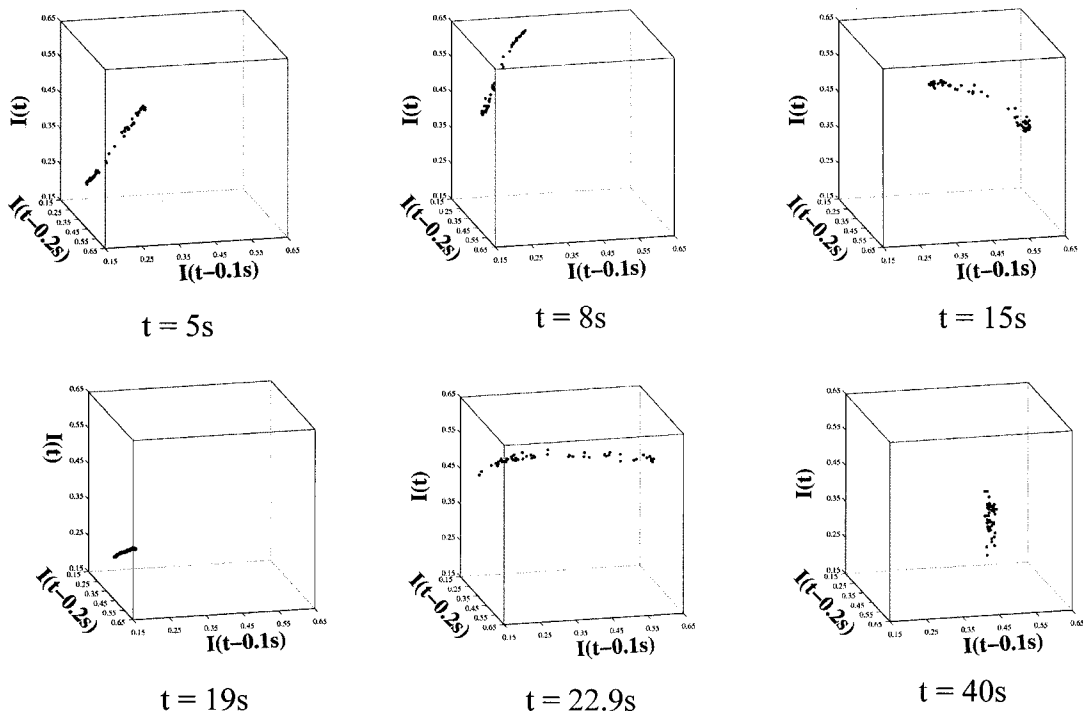


FIG. 7. Snapshots of position in state space for each of the 64 elements. Transient clusters at $\varepsilon = 0.78$.

more, the two clusters move relative to each other, that is they become closer and farther as time proceeds. Note, for example, that they are very close at $t = 8.6$. But there is no mixing of the elements; at times just after $t = 8.6$ s the two clusters move as entities away from each other.

A similar result is shown in Fig. 7 for the transient cluster region obtained at $\varepsilon = 0.78$. Note that two clusters sometimes form. This can be seen most easily in the figure at $t = 8$ s and $t = 15$ s. Sometimes, such as at $t = 19$ s, almost complete synchronization occurs. However, neither the clus-

ter formation nor the synchronization is stable. Both break up after a short time.

The difference between the currents of two electrodes in a transient cluster region is shown in Fig. 8. Note that the difference is sometimes large, on the order of the maximum attainable, and sometimes small, when the two elements are for a short time in an (unstable) cluster.

We have calculated the pair distances in three-dimensional state space between each set (i, j) of the 64 elements as a function of time. The pair distance is defined as

$$d_{i,j}(t) = \sqrt{(I(i,t) - I(j,t))^2 + (I(i,t - \Delta t) - I(j,t - \Delta t))^2 + (I(i,t - 2\Delta t) - I(j,t - 2\Delta t))^2}.$$

[There are $(64)(63)/2 = 2016$ such distances.] Normalized histograms of pair distance distributions (at $t = 20$ s, an arbitrarily chosen time) are presented in Fig. 9(a) for five values of the coupling parameter. At $\varepsilon = 0.0$ the pair distances are distributed fairly uniformly over a distance representative of the size of the attractor. At $\varepsilon = 1.0$ synchronization occurs and the pair distances are all small. At $\varepsilon = 0.725$ the two clusters are clearly seen. The other three parts of Fig. 9(a) represent either stable ($\varepsilon = 0.725$) or transient ($\varepsilon = 0.67$ and $\varepsilon = 0.78$) cluster behavior. We show some temporal dependence of the histograms in these regions in Figs. 9(b) and 9(c), respectively.

Pair distances in the stable cluster region are shown as a function of time in Fig. 9(b); it can again be seen that although the two clusters remain intact, the distance between them varies with time. Note, for example, that at $t = 8.6$ s the

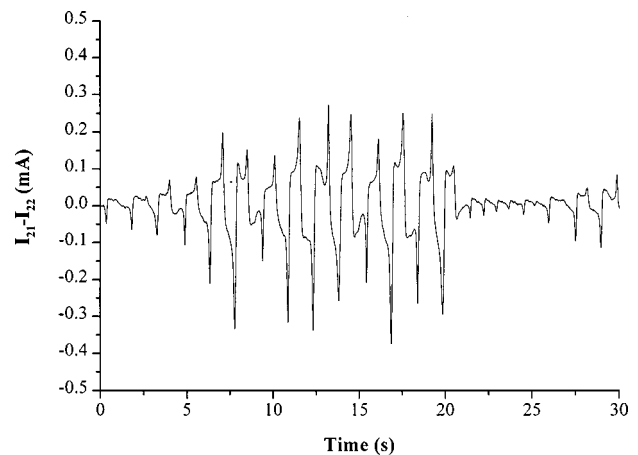
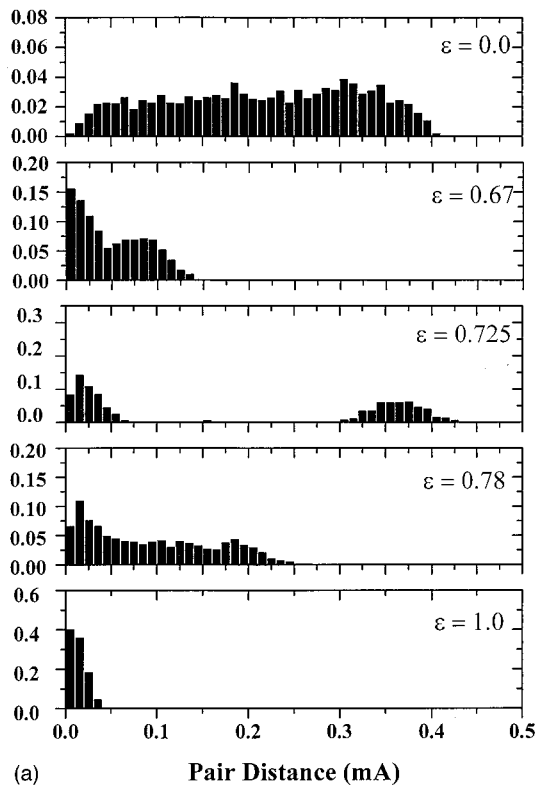
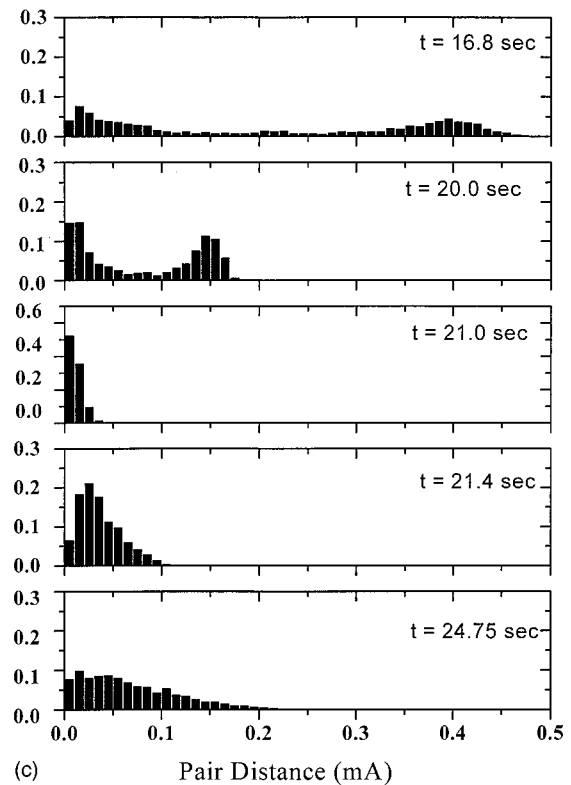


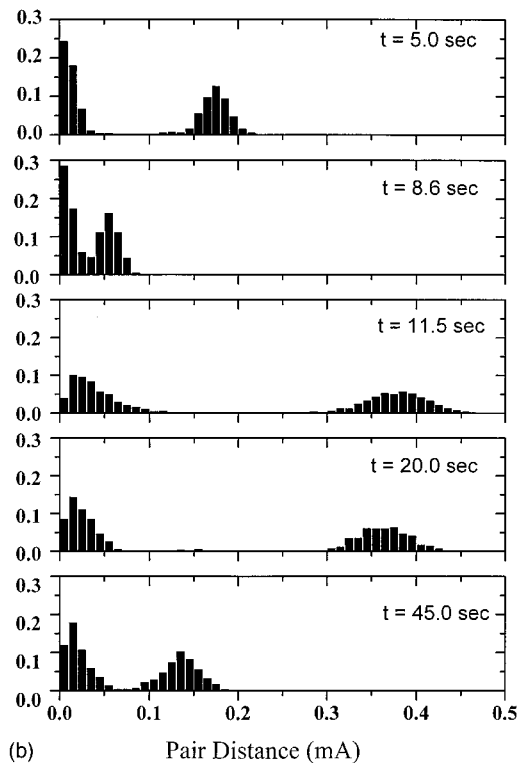
FIG. 8. Differences between currents on two electrodes. $\varepsilon = 0.67$, transient cluster region.



(a) Pair Distance (mA)



(c) Pair Distance (mA)



(b) Pair Distance (mA)

FIG. 9. Normalized histograms of pair distance distributions. (Snapshots). (a) Dependency on coupling strength. (b) Time dependency in cluster region, $\epsilon=0.725$. (c) Time dependency in a transient cluster region, $\epsilon=0.67$.

two clusters are very close together but that by $t=11.5$ s they have moved farther apart. Histograms of pair distances in one of the transient cluster regions ($\epsilon=0.67$) are shown in Fig. 9(c). Clusters do form (such as at $t=20$ s) and synchronization does occur (such as at $t=21$ s) but these states are not stable. At some times (such as at $t=16.8$ s) the distribution of pair distances is almost flat.

In order to characterize the synchronization and conden-

sation further we calculate an order parameter used previously by Zanette and Mikhailov in a study of coupled Rössler oscillators.¹¹ This order parameter is defined as the ratio of the number of pairs whose distance in three dimensional state space is less than some value, here taken to be 0.06 mA. (For numerical simulations with flows without noise and without heterogeneities, this distance can be taken to be zero.) The order parameter as a function of time is seen

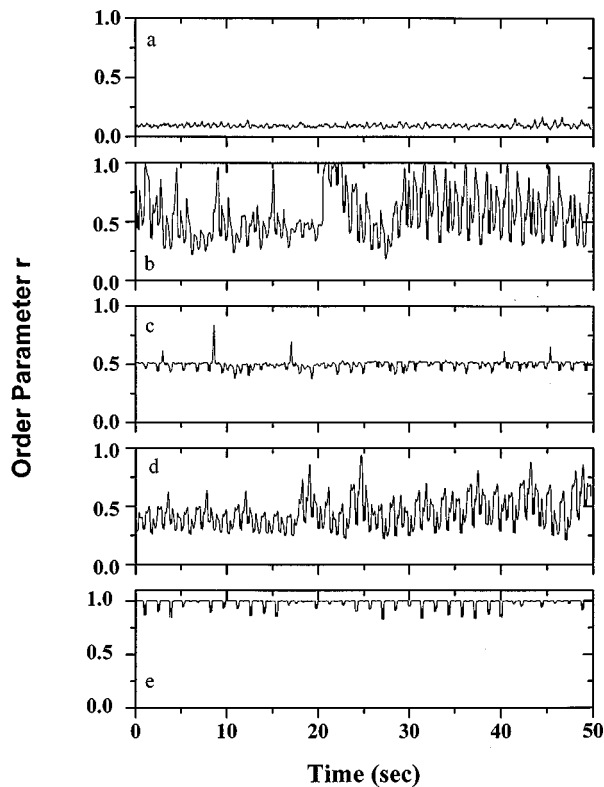


FIG. 10. Order parameter as function of time. (a) $\varepsilon=0$, (b) $\varepsilon=0.67$, (c) $\varepsilon=0.725$, for (23,41) cluster, (d) $\varepsilon=0.78$, (e) $\varepsilon=1.0$.

in Fig. 10 for several values of the coupling parameter. For $\varepsilon=0$ the order parameter is near zero at all times whereas at $\varepsilon=1.0$ it is near one. At $\varepsilon=0.725$, in the stable cluster region, the order parameter remains approximately constant at a value of 0.53. [For the results shown, which were calculated for a (23,41) cluster, the theoretical value of the order parameter in which all elements remain in their cluster for all times and when there is no overlap of clusters is $\{(23) \times (22)/2 + (41)(40)/2\} / \{(64)(63)/2\} = 0.53$.] The order parameter for the cluster region shown in Fig. 10 has occasional peaks to values well above the base line. This is not caused by experimental error but rather by the close approach of the two clusters. For example, consider the peak in the order parameter that occurs at $t=8.6$; this corresponds to the second panel of Fig. 6 in which the locations in state space are shown; note that the two clusters are close at this time. The peak in the order parameter occurs because the two clusters come close together and also, of course because we have taken a finite size sphere within which we define the elements to be together.

The order parameters for two of the transient cluster regions ($\varepsilon=0.67$ and $\varepsilon=0.78$) that occur on either side of the cluster region are also shown in Fig. 10. In both cases the order parameter goes through excursions above and below the value obtained for a two-cluster configuration. The order parameter for $\varepsilon=0.78$ corresponds to Fig. 7. Note that at $t=15$ s there are two (unstable) clusters and at $t=19$ s there is a short time of almost complete synchronization; the increase in order parameter as the synchronization occurs can be clearly seen as a peak in Fig. 10.

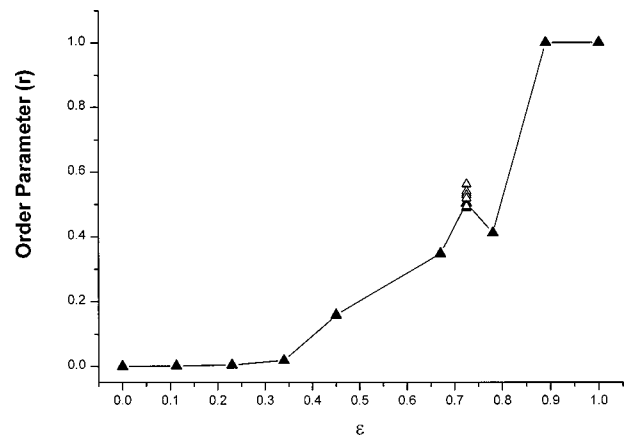


FIG. 11. Order parameter based on mean distances.

The variation in the order parameter as seen in Figs. 10(b) and 10(d) resembles the variation in the number of precision-dependent clusters seen by Kaneko in coupled maps. For example, note the description of chaotic itinerancy in Refs. 1 and 2 and Fig. 23 of Ref. 1. Note that the system described here varies from one with an almost completely uniform state, where the order parameter is approximately one, to one in which the order parameter takes on a very low value. This variation can also be seen in the state space plots, Fig. 7.

An order parameter as a function of coupling strength is shown in Fig. 11. This has been calculated by taking mean pair distances and calculating the order parameter from this mean. Obviously one can also calculate the order parameter at each time and take the mean of that, i.e., take the mean of the curves in Fig. 10. We found that the order parameter that we present here had the advantage of differentiating more clearly between clustered and nonclustered states and also shows more clearly the progression from a non-ordered to an ordered state. As seen in Fig. 11 the order parameter is zero at $\varepsilon=0$ and increases to 1.0 at $\varepsilon=1.0$. There is a maximum at the cluster region of $\varepsilon=0.725$. Obviously each cluster configuration has a different order parameter and these are also shown. Note that this is not experimental error, but is rather an indication that different order exists in different configurations. As defined, the order parameter increases as the number of elements in the larger cluster increases. Thus, the (32,32) cluster has the minimum order (0.49), (31,33) is slightly larger, etc.

IV. CONCLUDING REMARKS

We have designed an experimental chemically reacting system made up of individual elements to which global coupling can be added without changing other parameters of the system. When the global coupling is zero ($\varepsilon=0$), the other types of coupling inherent in the system were made small. The global coupling could thus be varied between a minimum where the oscillators had almost independent dynamics to a maximum where the oscillators were synchronized. The chaotic dynamics of the individual elements thus were

simple, that is, of low dimension, with no global coupling and with maximum coupling but were more complicated in intermediate regions.

Clustering occurs at intermediate values of the coupling parameter. We also observe transient cluster regions on both sides of the stable cluster region in which clusters form and total synchronization occurs but the clustering and synchronization are not stable. The attractors of the flows of the individual stable clusters had a two-band structure. Although we are dealing with an array of only 64 elements, we did see some of the same statistical properties seen by Zanette and Mikhailov in their simulations with globally coupled identical Rössler oscillators such as the pair distance distributions and variation of an order parameter.

We have observed only conditions with two stable clusters, although of course many such configurations exist at the same parameter values. The smallest number of elements in a cluster in the stable two-cluster region was 18, i.e., the observed range was from (18,46) to (32,32). It is possible to perturb the system from one stable configuration to another. Whether more clusters would be seen in an electrochemical system is not clear but we note that Kaneko has pointed out that two-cluster phase is associated with strong nonlinearities and coupling;³² the nonlinearities in the system being investigated are strong, notably the dependence of reaction rate on potential drop across the electrical double layer.

ACKNOWLEDGMENTS

This work was supported by the National Science Foundation and by the Fulbright Hungarian-American Exchange Program. We thank Professor A. Mikhailov for discussions and Professor K. Kaneko for helpful comments on the paper.

¹K. Kaneko, "Clustering, Coding, Switching, Hierarchical Ordering, and Control in a Network of Chaotic Elements," *Physica D* **41**, 137–172 (1990).

²K. Kaneko, "Globally coupled circle maps," *Physica D* **54**, 5–19 (1991).

³K. Kaneko, "Spatiotemporal Chaos in one- and two-dimensional coupled map lattices," *Physica D* **37**, 60–82 (1989).

⁴G. Perez, S. Sinha, and H. A. Cerdeira, "Order in the turbulent phase of globally coupled maps," *Physica D* **63**, 341–349 (1993).

⁵F. Xie and H. A. Cerdeira, "Coherent-ordered transition in chaotic globally coupled maps," *Phys. Rev. E* **54**, 3235–3238 (1996).

⁶G. Perez and H. A. Cerdeira, "Instabilities and nonstatistical behavior in globally coupled systems," *Phys. Rev. A* **46**, 7492–7497 (1992).

⁷W. Just, "On the collective motion in globally coupled chaotic systems," *Phys. Rep.* **290**, 101–110 (1997).

⁸A. Parravano and M. G. Cosenza, "Driven maps and the emergency of ordered collective behavior in globally coupled maps," *Phys. Rev. E* **58**, 1665–1671 (1998).

⁹S. C. Manrubia and A. S. Mikhailov, "Mutual synchronization and clus-

tering in randomly coupled chaotic dynamical networks," *Phys. Rev. E* (in press).

¹⁰D. H. Zanette and A. S. Mikhailov, "Mutual synchronization in ensembles of globally coupled neural networks," *Phys. Rev. E* **58**, 872–875 (1998).

¹¹D. H. Zanette and A. S. Mikhailov, "Condensation in globally coupled populations of chaotic dynamical systems," *Phys. Rev. E* **57**, 276–281 (1998).

¹²L. M. Pecora and T. L. Carroll, "Synchronization in chaotic systems," *Phys. Rev. Lett.* **64**, 821–824 (1990).

¹³L. M. Pecora, T. L. Carroll, G. A. Johnson, and D. Mar, "Fundamentals of synchronization in chaotic systems, concepts, and applications," *Chaos* **7**, 520–541 (1997).

¹⁴L. M. Pecora, "Synchronization conditions and desynchronizing patterns in coupled limit-cycle and chaotic systems," *Phys. Rev. E* **58**, 347–360 (1998).

¹⁵T. L. Carroll, J. F. Heagy, and L. M. Pecora, "Transforming signals with chaotic synchronization," *Phys. Rev. E* **54**, 4676–4680 (1996).

¹⁶J. F. Heagy, T. L. Carroll, and L. M. Pecora, "Synchronous chaos in coupled oscillator systems," *Phys. Rev. E* **50**, 1874–1885 (1994).

¹⁷M. G. Rosenblum, A. S. Pikovsky, and J. Kurths, "Phase synchronization of chaotic oscillators," *Phys. Rev. Lett.* **76**, 1804–1807 (1996).

¹⁸L. G. Brunnet and H. Chaté, "Phase coherence in chaotic oscillatory media," *Physica A* **257**, 347–356 (1998).

¹⁹Y. Kuramoto, *Chemical Oscillations, Waves and Turbulence* (Springer, Berlin, 1984).

²⁰I. Z. Kiss, W. Wang, and J. L. Hudson (unpublished).

²¹F. Mertens, R. Imbühl, and A. Mikhailov, "Turbulence and standing waves in oscillatory chemical reactions with global coupling," *J. Chem. Phys.* **101**, 9902–9908 (1994).

²²M. A. Liauw, M. Somani, J. Annamalai, and D. Luss, "Oscillating Temperature Pulses During CO Oxidation on a Pd/Al₂O₃ Ring," *AIChE J.* **43**, 1519–1528 (1997).

²³G. Flätgen and K. Krischer, "Accelerating fronts in an electrochemical system due to global coupling," *Phys. Rev. E* **51**, 3997–4004 (1995).

²⁴N. Mazouz, G. Flätgen, and K. Krischer, "Turning the range of spatial coupling in electrochemical systems: from local via nonlocal to global coupling," *Phys. Rev. E* **55**, 2260–2266 (1997).

²⁵P. Grauel, J. Christoph, G. Flätgen, and K. Krischer, "Stationary potential patterns during the reduction of peroxodisulfate at Ag ring electrodes," *J. Phys. Chem. B* **102**, 10264–10271 (1998).

²⁶J. Christoph, R. D. Otterstedt, M. Eiswirth, N. I. Jaeger, and J. L. Hudson, "Negative coupling during oscillatory pattern formation on a ring electrode," *J. Chem. Phys.* **110**, 8614–8621 (1999).

²⁷J. L. Hudson, in *Pattern Formation in Continuous and Coupled Systems*, IMA Volume in Mathematics and its Applications **115**, edited by M. Golubitsky, D. Luss, and S. H. Strogatz (Springer, Berlin, 1999), pp. 137–146.

²⁸R. D. Otterstedt, N. I. Jaeger, P. J. Plath, and J. L. Hudson, "Global coupling effects on spatiotemporal patterns on a ring electrode," *Chem. Eng. Sci.* **54**, 1221–1231 (1999).

²⁹Z. Fei and J. L. Hudson, "Chaotic oscillations on arrays of iron electrode," *Ind. Eng. Chem. Res.* **37**, 2172–2179 (1998).

³⁰Z. Fei, B. J. Green, and J. L. Hudson, "Spatiotemporal patterns on a ring array of electrodes," *J. Phys. Chem. B* **103**, 2178–2187 (1999).

³¹Z. Fei, R. Kelly, and J. L. Hudson, "Spatiotemporal patterns on electrode arrays," *J. Phys. Chem.* **100**, 18986–18991 (1996).

³²K. Kaneko, "Chaotic but regular Posi-Nega switch among coded attractors by cluster-size variation," *Phys. Rev. Lett.* **63**, 219–223 (1989).